Photo-thermal sensitive characters and reflective index variation of photo-thermo-reflective glass

DANCUI LI[a,b,*], WEINAN LI[a], MIN LU[a], PENGFEI WANG[a]
[a] *Institute of Advanced Materials (IAM), State Key Laboratory of Transient Optics and Photonics, Xi'an Institute of Optics and Precision Mechanics, Chinese Academy of Science (CAS), Xi'an, 710119, China*
[b] *Graduate University of Chinese Academy of Sciences, Beijing 100049, China*

The photo-thermo-reflective (PTR) glass is fabricated by the high temperature and melting process. The sample is characterized by differential scanning calorimetry (DSC), Ultraviolet- visible-near infrared spectroscopy, and X-ray diffraction (XRD). The experiment results show that NaF crystal is deposited in glass, the amount and the size of crystal phase precipitation can be achieved by controlling exposure dosage and time, thermal development temperature and time. At the same time, the reflective-index variation, about 5×10^{-4}, was measured by interference measuring method.

(Received October 11, 2012; accepted February 20, 2013)

Keywords: PTR glass, Exposure and thermal development, Reflective index variation

1. Introduction

In recent years, the volume grating ,which can be used to make diffractive elements such as spatial filters, attenuators, Bragg spectro- meters, and transverse and longitudinal mode selectors in a laser resonator [1], has attracted considerable attention due to the high diffraction efficiency, good angle and spectral selective [2]. At present, the main photo-sensitive materials [3] available for high-efficiency gratings recording are silver halide photographic emulsions, dichromated gelatin, photopolymers, and photo- refractive crystals. Each of these materials has its merits, but all the materials have some drawbacks. For example, organic materials are sensitive to humidity. Inorganic materials [4, 5] have low resistance to elevated temperatures and produce additional patterns because of exposure to the beam diffracted from the recorded grating. Owing to modulation of grating or record in surface of medium or limited to the properties of the recording medium, the properties of the grating is not robust, its application fields are very limited [6-8], especially the spatial filter of laser.

In order to overcome the problem, a new photosensitive material, named a photo-thermo- reflective (PTR) glass, is developed. PTR glass is a sodium-zinc-aluminum-silicate glass doped with silver, cerium and fluorine [9]. The photo- thermal process is based on precipitation of dielectric microcrystals in the bulk of glass exposed to UV radiation. The first stage is the exposure of the glass sample to the near UV radiation, which produces an ionization of a cerium ion, and then electrons released from the cerium are then trapped by silver ion converting them to neutral atom. This second stage is correspondence to a latent image formation in optical materials, and no significant coloration and refractive index variations occur in glass at this stage. The third stage is the diffusion of silver atoms, which leads that creation of tiny silver crystals begin growing. These silver particles serve as the nucleation centers for sodium fluoride crystal growth. After this stage, a refractive index of the exposed area in PTR glass became a few of fluctuation.

To our knowledge, a few comprehensive study of photo induced refraction in PTR glass has been undertaken [10], but the reflective index variation and the methods also need to further investigate. One of the problems that constrain these studies is the experimental difficulty of obtaining an accurate measurement of the induced refractive index in photosensitive media. A liquid-cell shearing interferometer, is so complex that the environment of match liquid can't be controlled, was adapted to measure reflective-index variation [11], so the most reliable method of induced refraction measure- ment is the interferometric one in which the Mach-Zehnder interferometer is used. In addition, test samples should be paid attention to choose that have less stripe and bubble parts; the most importantly, the test sample was processed perfectly and cut by cross section and then polished, the polished cross section would become the test sample surface, which can solve the problem and decrease surface imperfection caused phase shift. The problem a liquid-cell shearing interferometer method produced can be reduced and reflective-index variation can also be measured accurately in this way.

Efficient diffractive elements made of PTR glass have been demonstrated [12-14], experimental data concerning

on its crystalline phase precipitation characters has been undertaken and reported in the Ref. [10], but no integrated report on the optical-thermal sensitive characters. Thus our goal in the study is to concern on the optical-thermal sensitive characters of PTR glass and measuring reflective index variation in the PTR glass through post- treatment. Firstly, the sodium-zinc-aluminum- silicon PTR glass is fabricated by high temperature melting method. Then crystalli- zation tendency and internal phase composition of the glass by exposure and thermal develop- ment is analyzed by DSC and XRD, absorption respectively, which can comprehensively investigate the photo-thermal sensitive features of PTR glass. At last reflective index variation of the glass was measured by Mach-Zehnder interferometer.

2. Experimental

Sodium-zinc-aluminum-silicon is adopted as the host material, and a little photosensitive agent Ce^{3+} and photo-sensitizer Ag^{+} are introduced to the glass by form of CeO_2 and $AgNO_3$; joined halogen ion-$F^{-}$and Br^{-} that are added to the glass by form of KBr and NaF, they are the microcrystalline components after the light-thermal effect; and a little Sb_2O_3 and SnO, thermal-sensitive agents, which can make photo- chemical reaction rate of glass accelerant.

The glass was melted in an electrical furnace in 400 ml fused silica crucibles at 1460^{o}C for 5h. Stirring was applied to homogenize the melt. After the melting, the glass was cooled to the glass transition temperature in the open air by casting on to a thick metal slab or in the crucible. The glass casting (or boule) underwent annealing at 560℃for 2h and then cooled with a rate of 0.1℃/min in the region of structural and stress relaxation. Polished glass samples the similar thickness and size (15mm×15mm×7mm) samples were measured.

3. The results and discussion

3.1 Light-thermal mechanism of PTR glass

In order to confirm the thermal development system, no process glass powder is performed by the DSC STA 449 that is manufactured by Germany with a rate of 3℃/s temperature rise. Fig. 1 shows the exothermic peak at DSC curve.

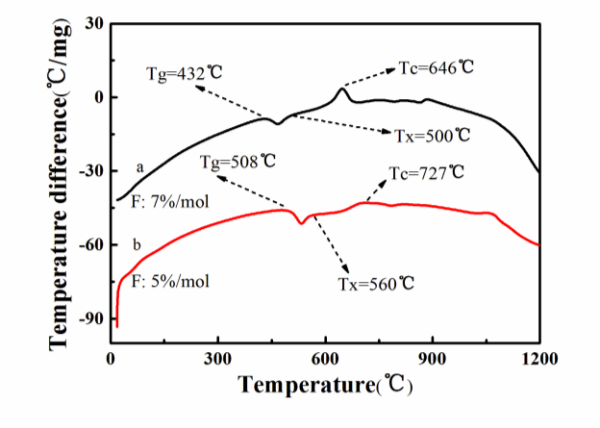

Fig. 1. (a), (b) the DSC curve of glass samples with different fluoride contain.

The samples of (a) and (b) have the different fluoride contain, we can gain the following results above the figure: The exothermic peak can be seen near 646 ^{o}C and 727 ^{o}C in heat enthalpy curve, so we can infer that peak of crystalline NaF precipitation of entire sample is on the temperature points, which can't correspond with our demand that the phase precipitation is produced partial glass; the glass transition temperature *Tg* is found at 432 ^{o}C and 508 ^{o}C, noteworthy, which is impacted by fluoride contain; the other temperature point *Tx* is about 500 ^{o}C and 560 ^{o}C in which the NaF crystal of partial glass (as confirmed by XRD, to be discussed in the following) began precipi- tating. Furthermore, one can also see that all temperature points of (b) are higher than (a), which results form different quantity fluoride. The much fluoride contain can improve microcrystalline property of glass, but excessive fluoride affect its thermal sensitive feature. Hence, the sample (b) is been adopted because its thermo stability is much stronger than sample (a). Consequently, the thermal development of PTR glass, connected with all glass crystallization temperature points of sample (b), is 460~520 ^{o}C and 500~560 ^{o}C respectively, it supplies assistance for following thermal development.

Then the samples were processed by exposure and thermal development according to table 1, sample b was treated by exposure 20s and thermal development 480 ^{o}C for 3h and 500 ^{o}C for 2h, sample c was treated by exposure 20s and thermal development 460 ^{o}C for 3h, 500 ^{o}C for 2h and 520 ^{o}C for 3h, the reason of which is to confirm thermal development temperature, because the DSC curve only demonstrated two temperature ranges and the accurate temperature was through the many experiments. Fig. 2 shows the changes of samples after different post- treatment, and thermal development process of sample (b) is shown in Fig. 3.

Table 1. Post-treatment for the samples.

sample	UV exposure	Condition of thermal development
a	0s	None
b	20s	480 °C for 3h,500 °C for 2h
c	20s	460 °C for 3h, 500 °C for 2h, 520 °C for 3h

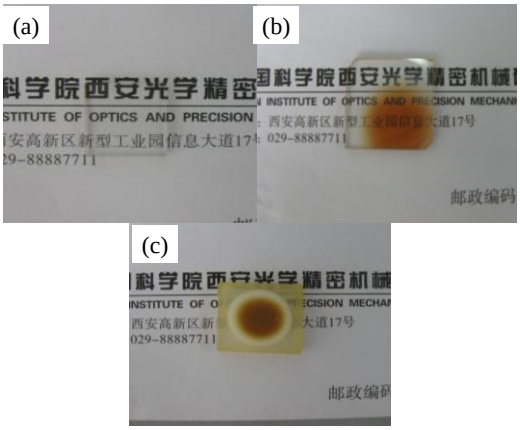

Fig. 2. Changes of the glass after different post-treatment: (a) virgin glass; (b) local exposure and low temperature thermal development; (c) local UV-exposure and high temperature thermal development.

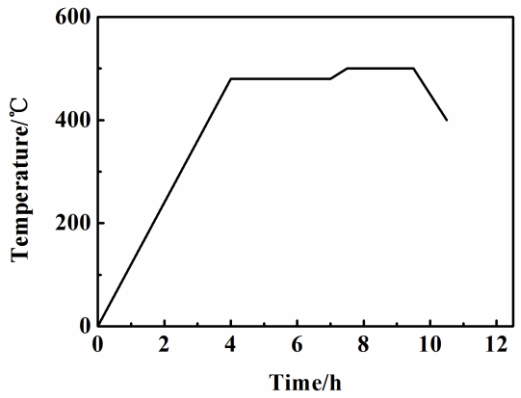

Fig. 3. Thermal development process of sample (b).

In the Fig. 2, coloration is produced in the samples undergoing these stages, photo-thermal sensitive mechanism, which can interpret as following: Ce^{3+} lose an electron that is captured by a silver ion Ag^{+} converting it to a neutral atom Ag^{0}; then corresponds to a latent image formation and no significant coloration exist; finally, the diffusion of silver atoms leads to creation of tiny silver containing particles and silver particles serve as the nucleation centers for sodium fluoride crystal growth.

In addition, one can also see from Fig. 2 (c) that part of the much exposure becomes into claybank, part of the less exposure is opaque white, and part of the un-exposure is light yellow. The reason of this phenomenon may be the part of much exposure dosage generated more nucleation, and then produced crystal particle smaller and much quantitative. When particle is small enough that visible light can be transmitted, it won't produce scattering. However, the part of less exposure dosage generated less nucleation, and then produced crystal particle bigger and less quantitative. When particle is big enough that visible light can't be transmitted, it will produce scattering. So the sample all is lost transparent and shelter from the background compared with sample (b) that its background is distinct and recognized. Furthermore, the above phenomenon also shows that we can make the microcrystal can be controllable by controlling the thermal development system.

3.2 Crystallization of PTR glass

In order to investigate the crystallization of PTR glass, the sample was exposed 20s and the thermal development temperature by sample (b) in the Table 1. Data were acquired by an X-ray diffract meter Rigaku model 'D/B max' with a CuK_a radiation and optimized operating conditions of 30mA and 35kV. All analyses presented in this paper were carried out at room temperature, scanning from 10° to 90° of 2Theta angle. Different scanning rates were studied to provide maximum sensitivity of the method of the crystalline admixture detection.

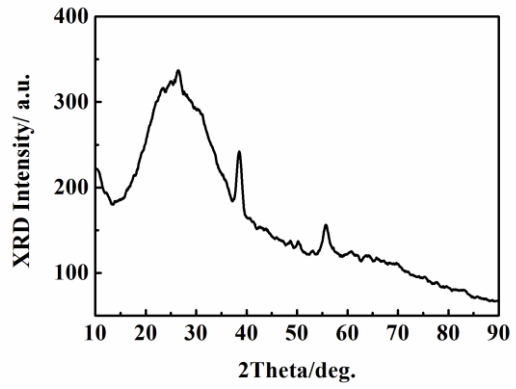

Fig. 4. XRD pattern of the glass after post-treatment.

Previous experiments demonstrate that crystallization tendency of the glass is ascribed to contain fluorine. The more fluorine contains, the more crystallization tendency produces. Fig. 4 shows X-ray diffraction (XRD). The main value of the wider peak is 23 degree from 15 degree to 40 degree, which is intrinsic peak of the silicate glass. One can see the three sharp peaks match with the expected NaF Villaumite crystalline phase located at 39°, 56° and 70.5°

as was described and the Fig. 4 and in earlier works [15-19]. However, a weak singularity that can be classified as a small peak also can be found in the region of 30° which is a signature of NaBr. These data mean that the main crystalline phase precipitated in PTR glass is NaF with possible small admixture of NaBr. No other crystalline phases detectable by XRD were found in totally crystallized PTR glass samples. It should be noted that a bright yellow residue was precipitated on the abraded surfaces of thermally treated samples which could be due to a silver containing compound. However, we did not study this surface phenomenon in the current work. Thus, the main crystalline phase precipitating in the unexposed PTR glass after thermal treatment is a cubic NaF one.

To determine further the crystallization of PTR glass, the samples were exposed 20s and 50s and the thermal development temperature by sample (b) in the Table 1. Fig. 5 displays the absorption spectrum of PTR glass that is measured by UV-3101 (pc) instrument of SHIMADZU made in Japan from ultraviolet area to visible area. Induced absorptions were described in the following. An absorption peak of glass undergoing UV exposure is in the UV region. Thermal development causes an additional absorption in the visible region. Colorless fluoride crystals cannot cause an additional absorption but they can produce an induced scattering. Colloidal particles of silver and silver halides are responsible for additional absorption band in the blue region.

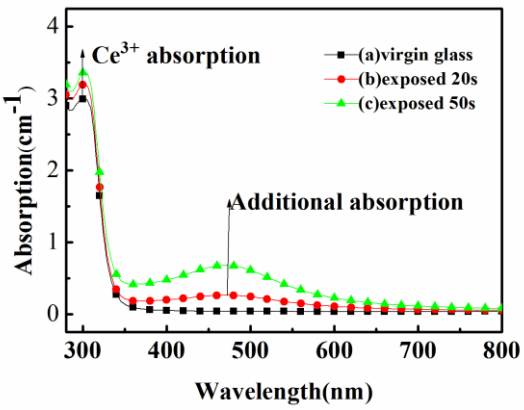

Fig. 5. UV-visible absorption spectrums of the glass: (a) virgin glass, (b) exposure: 20s, (c) exposure: 50s.

One can see the wide absorption band of Ce^{3+} with a maximum at 305nm, which can be regard as the intrinsic absorption of PTR glass. From the point of view of technical application, the short-wavelength edge, at which the writing radiation is attenuated by two times in the recording medium, is placed at 330 nm for a 1-cm-thick plate and at 265 nm for 1-mm-thick plate. The range of photosensitivity of this glass is from 280 to 360 nm.

Detectable photoinduced absorption is seen only in the UV region. Even at the recording wavelength, the absorption is so small that cannot impact the recording process significantly. The small tail of the induced absorption spectrum in the blue region can be distinguished by the naked eye as a slight yellow coloration of the exposed area. Thermal development causes colloidal Ag and NaF precipitation in the glass matrix. Fluoride crystals are colorless but can result in scattering if the size of the crystals is too large (more than 100nm [20]). A shoulder near 470 nm in the additional absorption spectrum after thermal treatment was ascribed to silver particles in the glass matrix. In addition, the reason that bend of the curve (c) near the 470nm is the bigger than curve (b) is relation to the exposure time, actually the exposure dosage, so growth of the NaF crystal particles were different after the heat treatment. The virgin glass don't emerge absorption in visible area also can interpret above phenomenon. Therefore, the absorption is produced due to the exposure time superficially, but the exposure dosage, so we control the exposure dosage by the exposure time.

3.3 Measure of refractive index variation

According to the different interference fringes sample has effect on optical path. By this method, the refractive index variation is calcul- ated. The main problems of effects on the interference are uneven surfaces and phase distortions, especially when the surface imper- fection caused phase shift is comparable with the phase shift originate from the refractive-index variation. The test sample surface was described in Fig. 6 by microscope and the thickness is 0.5 mm.

The interference fringes can emerge distortions and movement in adding the test sample, change of phase can be calculated by calculating the number of fringes movement. And fringes move one correspondingly when optical path varies a λ/2 distance in light path; that is

$$\Delta n * t = \Delta s * \lambda / 2 \tag{1}$$

So, we can obtain the formula of refractive index variation, following as:

$$\Delta n = \lambda * \Delta s / 2t \tag{2}$$

Where Δs is the number of fringes movement, t is the thickness of the glass.

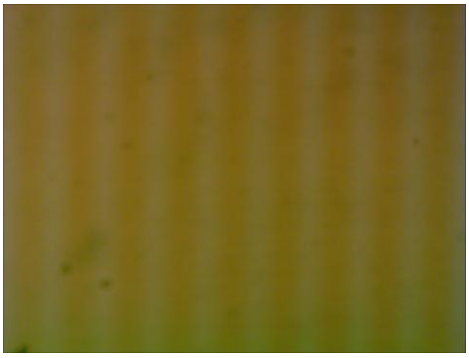

Fig. 6. The test sample of recording grating in interior of glass.

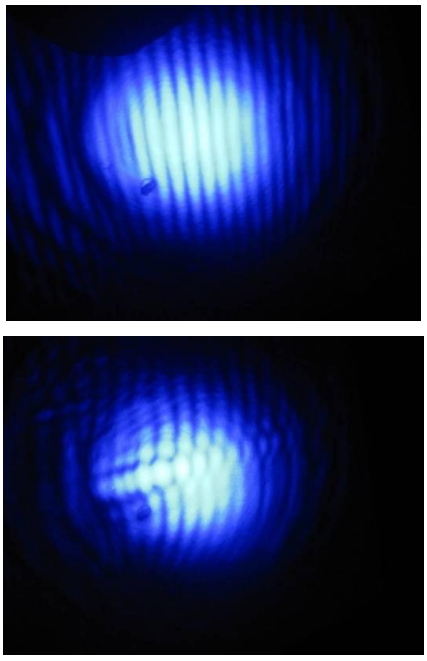

Fig. 7. Interference fringes of experiment scheme: (a) interference fringes of no sample; (b) interference fringes of sample.

According to the above Fig. 7, one can see that the fringes move one towards the left, the interference fringes that were imaged in the CCD were observed by CCD system, the refractive-index variation can be calculated according to the formula:

$$\Delta n = \lambda * \Delta s / 2t$$

$$= 515\times10^{-6} * 1/ (2\times0.5) \approx 5\times10^{-4}$$

Consequently, refractive-index variation of PTR glass is about 5×10^{-4}, the volume Bragg grating recording in which can be used the spatial filter of laser.

4. Conclusions

In summary, a PTR glass has been fabricated and its photo-thermal sensitive characters were comprehensive researched. DSC indicated the thermal development system and processes including two steps: nucleation and crystallization, so temperature range is detected 460~520℃ and 500~560℃ respectively; and we can control process of crystal phase precipitation in the glass by controlling exposure dosage and conditions of heat treatment. After the process, the sample is coloration; a refractive index of the exposed area in PTR glass became a few of fluctuation; and NaF crystal phase precipitation, companied a very small part of the NaBr, can be detected by XRD. An additional absorption is generated near 470nm from the absorption spectrum, and the absorption of PTR glass is small from ultraviolet to visible area, so the working band is wide. At last reflective-index variation measured about 5×10^{-4} in exposed area of PTR glass sample by interference, the volume Bragg grating was recorded in the glass interior can be used in the spatial filter of laser.

Acknowledgement

This work was supported by West Light Foundation of the Chinese Academy of Sciences (No.Y129261213) and the National Nature Science Foundation of China (No.51002181), which is gratefully acknowledged.

References

[1] M. Demenikov, J. Lumean, V. K. Rotar, A. Sevian, V. I. Smirnov, L. B. Glebov, Proc. SPIE 6216, 62160Y (2006).
[2] M. Efimov, L. B. Glebov, L. N. Glebova, K. C. Richardson, V. I. Smirnov, Appl. Optics, Optical Technology and Biomedical Optics (OT&BO), **38**, 619-627.182 (1999).
[3] P. Hariharan, Principles, Techniques, and Applications (Cambridge U. Press, Cambridge, UK, 1996), Chap. 7, pp. 95-124.
[4] L. B. Glebov, N. V. Nikonorov, et al., Opt. Spectrosc. **73**, 237 (1992).
[5] O. M. Efimov, L. B. Glebov, L. N. Glebova, V. I. Smirnov. United States Patent 6, 586, 141 (2003).
[6] L. B. Glebov, N. V. Nikonorov, E. I. Panysheva, G. T. Petrovskii, V. V. Savvin, I. V. Tunimanova, V. A. Tsek-homskii, Sov. Phys. Dokl. **35**, 878 (1990).
[7] L. B. Glebov, N. V. Nikonorov, E. I. Panysheva, G. T. Petrovskii, V. V. Savvin, I. V. Tunimanova, V. A. Tsek-homskii, Opt. Spectrosc. **73**, 237 (1992).
[8] S. D. Stookey, Ind. Eng. Chem. **41**, 856 (1949).
[9] L. B. Glebov, V. I. Smirnov, C. M. Stickley, I. V. Ciapurin, in Laser Weapons Technology III, W. E. Thompson and P. H. Merritt, Eds., Proc. SPIE, **4724**,

101 (2002).
[10] T. Cardinal, O. M. Efimov, H. G. Francois-Saint-Cyr, L. B. Glebov, L. N. Glebova, V. I. Smirnov, Journal of Non-Crystalline Solids **325**, 275 (2003).
[11] Oleg M. Efimov, Leonid B. Glebov, Herve ´ P. Andre, Applied Optics (Optical Society of America 2002).
[12] L. B. Glebov, N. V. Nikonorov, E. I. Panysheva, G. T. Petrovskii, V. V. Savvin, I. V. Tunimanova, V. A. Tsekhomskii, Opt. Spectrosc. **73**, 237 (1992).
[13] O. M. Efimov, L. B. Glebov, L. N. Glebova, V. I. Smirnov. United States Patent 6, 586, 141, 2003.
[14] O. M. Efimov, L. B. Glebov, V. I. Smirnov. U. S. Patent 6, 673, 497 (2004).
[15] S. D. Stookey, G. H. Beall, J. E. Pierson, J. Appl. Phys. **49**, 5114 (1978).
[16] V. V. Astakhova, N. V. Nikonorov, E. I. Panysheva, V. V. Savvin, I. V. Tunimanova, V. A. Tsekhomskii, Sov. J. Glass Phys. Chem. **18**, 152 (1992).
[17] E. V. Anoshkina, I. A. Evdoseeva, E. I. Panysheva, I. V. Tunimanova, Glass Phys. Chem. **20**, 33 (1994).
[18] E. I. Panysheva, I. V. Tunimanova, Glass Phys. Chem. **22**, 125 (1996).
[19] N. V. Nikonorov, E. I. Panysheva, I. V. Tunimanova, A. V. Chukharev, Glass Phys. Chem. **27**, 241 (2001).
[20] A. V. Dotsenko, A. M. Efremov, V. K. Zakharov, E. I. Pany-sheva, I. V. Tunimanova, Sov. J. Glass Phys. Chem. **11**, 592 (1985).

*Corresponding author: lidancui0128@126.com